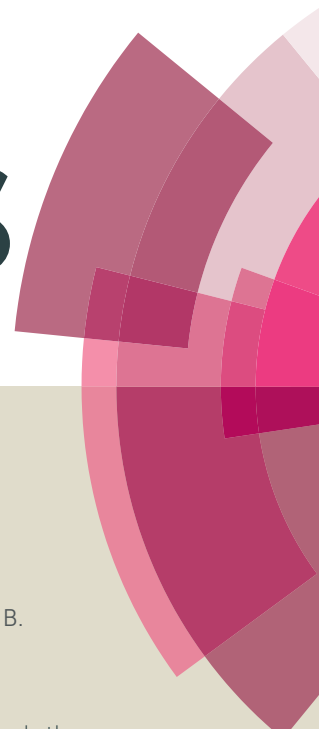


RSC Advances



This article can be cited before page numbers have been issued, to do this please use: Z. Cong, S. Liu, B. Zhao, W. Wang, H. Liu, J. Su, Z. Guo, W. Wei, C. Gao and Z. An, *RSC Adv.*, 2016, DOI: 10.1039/C6RA13595A.



This is an *Accepted Manuscript*, which has been through the Royal Society of Chemistry peer review process and has been accepted for publication.

Accepted Manuscripts are published online shortly after acceptance, before technical editing, formatting and proof reading. Using this free service, authors can make their results available to the community, in citable form, before we publish the edited article. This *Accepted Manuscript* will be replaced by the edited, formatted and paginated article as soon as this is available.

You can find more information about *Accepted Manuscripts* in the [Information for Authors](#).

Please note that technical editing may introduce minor changes to the text and/or graphics, which may alter content. The journal's standard [Terms & Conditions](#) and the [Ethical guidelines](#) still apply. In no event shall the Royal Society of Chemistry be held responsible for any errors or omissions in this *Accepted Manuscript* or any consequences arising from the use of any information it contains.



Journal Name

ARTICLE

High Performance Alternating Polymers Based on Two-dimensional Conjugated Benzo[1,2-b:4,5-b']dithiophene and Fluorinated Dithienylbenzothiadiazole for Solar Cells[†]

Zhiyuan Cong,^{a,b,†} Shuo Liu,^{c,†} Baofeng Zhao,^{a,b} Weiping Wang,^{a,b} Hongli Liu,^{a,b} Jin Su,^a Zhaoqi Guo,^a Wei Wei,^c Chao Gao,^{a,b,*} Zhongwei An^{a,b,*}

Received 00th January 20xx,
Accepted 00th January 20xx

DOI: 10.1039/x0xx00000x

www.rsc.org/

Three donor-acceptor polymers based on two-dimensional conjugated alkylthienyl substituted benzo[1,2-b:4,5-b']dithiophene (BDTT) and fluorinated 4,7-dialkylthienyl-2,1,3-benzothiadiazole (DTBT) derivatives were synthesized and applied as donor materials for bulk heterojunction solar cells. The effects of fluorine substitution on the absorption properties, energy levels, dielectric constants and photovoltaic properties of the polymers were investigated. We found that the incorporation of fluorine atoms on the DTBT unit can effectively deepen the highest occupied molecular orbital (HOMO) energy level and increase the dielectric constant of the polymers. As a result of these improved properties, a high open-circuit voltage (V_{oc}) of 0.85V was obtained for the optimal conventional polymer solar cells (PSCs) based on a two-fluorine-substituted analogue **P3** blended with [6,6]-phenyl-C71 butyric acid methyl ester (PC₇₁BM) as the active layer (1:1.5), giving rise to a high power conversion efficiency (PCE) of 7.48%. The influences of the molecular weight (MW) of **P3** on the device performances were further studied and enhanced photovoltaic parameters were achieved for the medium molecular weight **P3** based device, with corresponding open circuit voltage (V_{oc}) of 0.80 V, short-circuit current density (J_{sc}) of 14.7 mA cm⁻², high fill factor (FF) of 71.9% and the resulting best PCE of 8.47%, verifying that **P3** with appropriate MW should be promising polymer for highly efficient photovoltaic application.

1. INTRODUCTION

Recently, polymer solar cells (PSCs) have achieved tremendous progresses, resulting in the realization of above 10% power conversion efficiency (PCE) in single active layer devices.^[1-4] The progresses were not only ascribed to the comprehensively understanding and control of charge generation and transportation in the devices, but also due to the intense research efforts devoted to finely design and tailor novel donor materials, especially the rapid development of novel alternating donor-acceptor (D-A) conjugated polymers. In the past decade, numerous studies had proven that the photoelectric properties of these D-A conjugated polymers can be finely tuned by controlling the photo-induced intermolecular charge transfer (ICT) from D to A units, rendering them with suitable bandgaps and low-lying highest

occupied molecular orbital (HOMO) energy levels. Therefore, this strategy has become one of the most successful method to prepare desire polymers to deliver both high short-circuit current density (J_{sc}) and open-circuit voltages (V_{oc}).^[5,6]

Among a great variety of novel alternating D-A polymers, the most widely used D segments are fluorene (FO), carbazole (C₂), dithieno[3,2-b:2',3'-d]-silole (DTS), indacenodithiophene (IDT), benzo[1,2-b:4,5-b']dithiophene (BDT), *etc.*,^[5,7] while the A moieties are usually chosen from quinoxaline (Qx), pyrrolo[3,4-c]-pyrrole-1,4-dione (DPP), thieno(3,4-b)thiophene (TT), 4,7-di(thien-2-yl)-2,1,3-benzothiadiazole (DTBT), *etc.*^[8] Based on this strategy and arrangement, many polymers have been designed and used as electron donor materials for highly efficient photovoltaic devices. Owing to their planar and rigid geometry and facile synthesis routine with high yield, BDT and DTBT derivatives are promising electron-rich and electron-withdrawing units to construct high performance alternating polymers for photovoltaic application. Numerous polymers based on BDT and DTBT with optimized structures and side chains have been reported.^[9-18] To date, a BDT and fluorinated benzothiadiazole based polymer with bulk branched alkoxy side chains in BDT segment delivered one of the highest PCE of 8.30%,^[17] mainly due to the improved processability and J_{sc} .

In comparison with alkyl substituted BDT derivatives, the thienyl-substitution in the 4,8-positions of BDT unit is beneficial to broaden the absorption band, lower the HOMO level and improve the hole mobility of the resulting

^a State Key Laboratory of Fluorine & Nitrogen Chemicals, Xi'an, Shaanxi, 710065, P.R.China.

^b Xi'an Modern Chemistry Research Institute, Xi'an, Shaanxi, 710065, P. R. China. E-Mail: chaogao1974@hotmail.com (C. Gao), gmecazw@163.com (Z. An).

^c Institute of Advanced Materials, Nanjing University of Posts and Telecommunications, Nanjing 210003, P. R. China.

[†] These authors contributed equally to this work.

[‡] Electronic Supplementary Information (ESI) available: Absorption spectra and photovoltaic performances polymer **P3** with different MW. This material is available free of charge via the Internet at <http://pubs.acs.org>. See DOI: 10.1039/x0xx00000x

copolymers. Previously alkylthienyl substituted BDT (BDTT) were designed as electron-rich units for construction of two-dimensional (2D) conjugated polymers with a variety of electron-withdrawing units for high performance photovoltaic devices.^[9,19-21] However, the power conversion efficiency (PCE) of the alternating polymers based on BDTT and DTBT derivatives are unsatisfactory to some extent,^[10,17,18] mainly due to the poor solubility and processability of the 2D planar conjugated polymer. Therefore, to further modification of the side chain both in DTBT and BDTT segments are necessary to improve performance of this type of polymers.

In this paper, we report the synthesis and photovoltaic behaviour of three alternating polymers based on BDTT and DTBT derivatives, namely poly{4,8-di(2,3-dioctylthiophene-5-yl)-2,6-benzo[1,2-b:4,5-b']dithiophene-*alt*-4,7-di(4-hexylthiophen-2-yl)-2,1,3-benzothiadiazole} (**P1**), poly{4,8-di(2,3-dioctylthiophene-5-yl)-2,6-benzo[1,2-b:4,5-b']dithiophene-*alt*-4,7-di(4-hexylthiophen-2-yl)-5-fluorine-2,1,3-benzothiadiazole} (**P2**), poly{4,8-di(2,3-dioctylthiophene-5-yl)-2,6-benzo[1,2-b:4,5-b']dithiophene-*alt*-4,7-di(4-hexylthiophen-2-yl)-5,6-difluorine-2,1,3-benzothiadiazole} (**P3**). The structures of the three polymers were shown in **Scheme 1**. According to our previous work,^[21] the dioctylthienyl groups that introduced onto the BDT unit to build the 2D conjugated polymers, could effectively improve the solubility and lower the HOMO energy levels. Additionally, thiophene with hexyl substituent was inserted as the spacer in between the benzo[1,2-b:4,5-b']dithiophene and benzothiadiazole segment to expand the conjugating degree and modulate the solubility of the polymers. Moreover, one or two fluorine atoms were taken in the benzothiadiazole units to tune the HOMO energy levels and the relative dielectric constant (ϵ), which would facilitate the V_{oc} of the polymers.^[22] We found the difluoro polymer **P3** with medium molecular weight (MW) based conventional device displayed the highest PCE of 8.47% and should be promising for highly efficient photovoltaic application.

2. EXPERIMENTAL SECTION

2.1 Materials

Unless otherwise noted, all chemicals and reagents are obtained from Aldrich or Alfa & Aesar. Tetrahydrofuran (THF) and diethyl ether are dried over Na/benzophenone ketyl and freshly distilled prior to use. Other materials were used as received without further purification. The monomers 2,6-bis(trimethyltin)-4,8-bis(2,3-(dioctyl)thiophen-5-yl)-benzo[1,2-b:4,5-b']dithiophene (**M1**),^[19,21] 4,7-di(4-hexyl-5-bromo-thiophen-2-yl)-2,1,3-benzothiadiazole (**M2**), 4,7-di(4-hexyl-5-bromo-thiophen-2-yl)-5-fluorine-2,1,3-benzothiadiazole (**M3**) and 4,7-di(4-hexyl-5-bromo-thiophen-2-yl)-5,6-difluorine-2,1,3-benzothiadiazole (**M4**)^[9-11] were prepared using the literature procedures with some modifications.

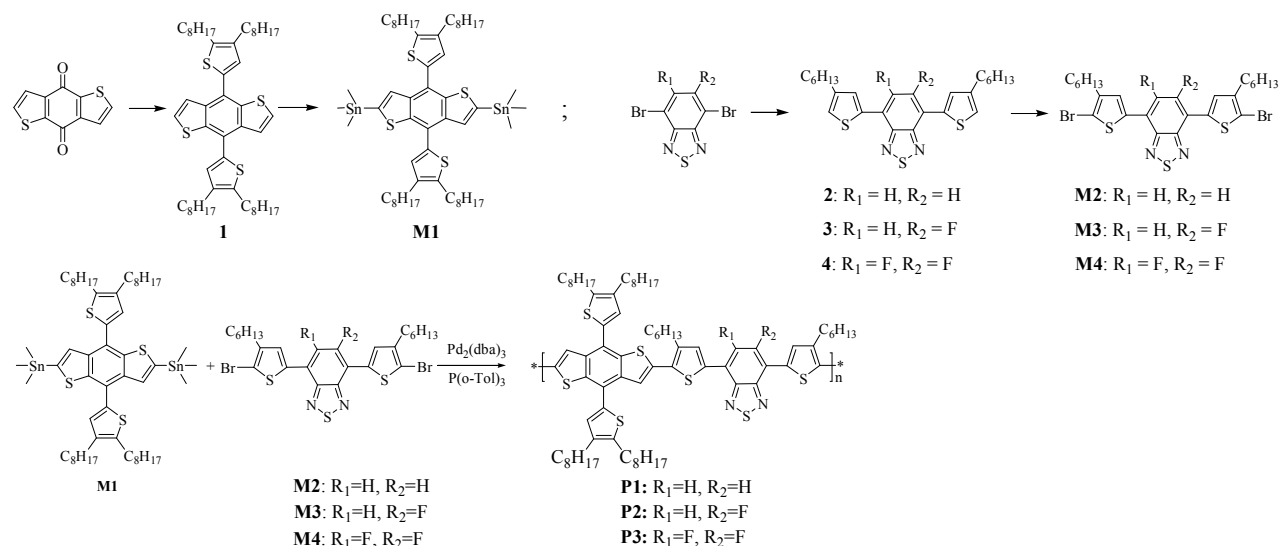
4,8-bis(2,3-(dioctyl)thiophen-5-yl)-benzo[1,2-b:4,5-b']dithiophene (Compound 1). 2,3-dioctylthiophene (12.34 g, 40 mmol) was dissolved in anhydrous THF (120 ml) under nitrogen, the solution was cooled to 0 °C in an ice water bath, and n-BuLi (2.5 M, 40 mmol) was added dropwise slowly to the mixture, then the reaction was heated to 50 °C and kept at this temperature for 1 h. Subsequently, 4,8-dehydrobenzo[1,2-b:4,5-b']dithiophene-4,8-dione (3.10 g, 14.44 mmol) was added and the mixture was stirred at 50 °C for another 2 h. Then the reaction was cooled down to room temperature, a solution of SnCl₂·2H₂O (26 g, 115.04 mmol) in 10% HCl (34 ml) was added, and the reaction was further stirred for 2 h. The resulting mixture was extracted with diethyl ether and the organic layer was washed with water and dried over MgSO₄. After evaporated to remove the solvent, the crude was purified by silica gel chromatography, using hexane as eluent to obtain **compound 1** as a viscous liquid (5.66g, 48.8 %). ¹H NMR (CDCl₃, 500MHz) δ (ppm): 7.70 (d, 2H), 7.45 (d, 2H), 7.22 (s, 2H), 2.82 (t, 4H), 2.61 (t, 4H), 1.73 (dt, 4H), 1.65 (dt, 4H), 1.39 (m, 40H), 0.90 (td, 12H). ¹³C NMR (CDCl₃, 125 MHz) δ (ppm): 140.19, 138.84, 138.13, 136.35, 135.08, 129.86, 127.29, 124.13, 123.61, 77.29, 77.04, 76.79, 31.95, 31.93, 31.88, 30.87, 29.57, 29.55, 29.44, 29.38, 29.31, 28.34, 28.03, 22.74, 14.25.

2,6-Bis(trimethyltin)-4,8-bis(2,3-(dioctyl)thiophen-5-yl)-benzo[1,2-b:4,5-b']dithiophene (M1). **Compound 1** (4.0 g, 5 mmol) was dissolved in anhydrous THF (40 ml) under nitrogen. The mixture was cooled to 0 °C and n-BuLi (2.5 M, 12 mmol) was added dropwise slowly to the mixture. Then the reaction was kept at 0 °C for 1 h, SnMe₃Cl (2.75 g, 13.8 mmol) was added quickly in one portion at 0 °C, then the mixture was warmed to room temperature and stirred for another 0.5 h. The reactant was poured into water and extracted with diethyl ether, the organic layer was washed with water and dried over MgSO₄, then evaporated to remove the solvent. The residue was recrystallized with THF/isopropanol for several times to obtain **M1** as a faint yellow crystal (3.22 g, 56.9%). ¹H NMR (CDCl₃, 500MHz) δ (ppm): 7.73 (s, 2H), 7.23 (s, 2H), 2.84 (t, 4H), 2.62 (m, 4H), 1.75 (dt, 4H), 1.67 (m, 4H), 1.46 (dt, 8H), 1.34 (m, 32H), 0.89 (m, 12H), 0.40 (m, 18H). ¹³C NMR (CDCl₃, 125 MHz) δ (ppm): 139.81, 137.99, 137.18, 135.76, 131.42, 129.82, 122.49, 31.97, 31.91, 31.84, 30.85, 29.62, 29.53, 29.46, 29.35, 29.32, 28.34, 28.05, 22.70, 14.14, -6.87, -6.94, -8.35, -9.76, -9.82.

4,7-di(4-hexyl-thiophen-2-yl)-2,1,3-benzothiadiazole (Compound 2). 4,7-dibromo-2,1,3-benzothiadiazole (2.9 g, 9.7 mmol) and 2-tributyltin-4-hexyl-thiophene (21g, 24.2 mmol) were dissolved in anhydrous THF (60 ml) under nitrogen. The catalyzer Pd(PPh₃)₂Cl₂ (0.13 g) was added. Then the solution was heated to reflux overnight. When cooled down to ambient temperature, the solution was poured into water. The organic phase was extracted with diethyl ether and dried over MgSO₄, then evaporated to obtain an orange powder. The crude was purified by silica gel chromatography using hexane as eluent to obtain **compound 2** as orange powder (3.7 g, 88%). ¹H NMR (500 MHz, CDCl₃): δ (ppm) 7.95 (s, 2H), 7.77 (s, 2H), 7.02 (s, 2H),

Journal Name

ARTICLE



Scheme 1 Synthetic route and molecular structures of the monomers and polymers

2.68 (t, 4H), 1.69 (t, 4H), 1.29-1.42 (m, 12H), 0.90 (t, 6H). ¹³C NMR (125 MHz, CDCl₃): δ(ppm) 152.62, 144.35, 139.03, 129.00, 125.99, 125.49, 121.52, 31.75, 30.69, 30.50, 29.10, 22.68, 14.15.

4,7-di(4-hexyl-thiophen-2-yl)-5-fluorine-2,1,3-benzothiadiazole (Compound 3). This monomer was synthesized according to the similar route as **compound 2** with a yield as 3.6 g (77%). ¹H NMR (500 MHz, CDCl₃): δ(ppm) 8.09 (s, 1H), 7.97 (s, 1H), 7.72 (d, 1H), 7.14 (s, 1H), 7.08 (s, 1H), 2.70 (m, 4H), 1.70 (m, 4H), 1.25-1.41 (m, 12H), 0.90 (t, 6H). ¹³C NMR (125 MHz, CDCl₃): δ(ppm) 159.89, 157.87, 153.56, 149.79, 144.52, 143.49, 137.61, 132.17, 131.50, 129.85, 125.90, 122.89, 116.70, 110.20, 31.72, 30.61, 30.55, 30.47, 29.05, 22.65, 14.12.

4,7-di(4-hexyl-thiophen-2-yl)-5,6-difluorine-2,1,3-benzothiadiazole (Compound 4). This monomer was synthesized according to the similar route as **compound 2** with a yield as 1.3 g (61%). ¹H NMR (500 MHz, CDCl₃): δ(ppm) 8.09 (s, 2H), 7.18 (s, 2H), 2.70 (t, 4H), 1.70 (m, 4H), 1.32-1.35 (m, 12H), 0.90 (t, 6H). ¹³C NMR (125 MHz, CDCl₃): δ(ppm) 150.80, 148.87, 143.68, 132.25, 131.21, 123.92, 110.65, 31.72, 30.52, 30.49, 29.05, 22.66, 14.12.

4,7-di(4-hexyl-5-bromo-thiophen-2-yl)-2,1,3-benzothiadiazole (M2). **Compound 2** (3.9 g, 8.43 mmol) and NBS (3g, 16.9 mmol) were dissolved in DMF (130 mL) and then heated to 60 °C for 3 h. When cooled down to ambient temperature, the solution was poured into methanol. The crude was collected by filtration and recrystallized with hexane/isopropanol for three times to give the target monomer **M2** as a orange crystal (0.6 g, 47%). ¹H NMR (500

MHz, CDCl₃): δ(ppm) 7.77 (s, 2H), 7.74 (s, 2H), 2.65 (t, 4H), 1.68 (m, 4H), 1.25-1.41 (m, 12H), 0.90 (t, 6H). ¹³C NMR (125 MHz, CDCl₃): δ(ppm) 152.21, 143.07, 138.50, 128.06, 125.28, 124.81, 111.61, 31.65, 29.75, 29.69, 28.97, 22.63, 14.11.

4,7-di(4-hexyl-5-bromo-thiophen-2-yl)-5-fluorine-2,1,3-benzothiadiazole (M3). **M3** was synthesized according to the similar route as **M2** with a yield as 3.7 g (70%). ¹H NMR (500 MHz, CDCl₃): δ(ppm) 7.95 (s, 1H), 7.75 (s, 1H), 7.66 (d, 1H), 2.66 (m, 4H), 1.68 (m, 4H), 1.32-1.41 (m, 12H), 0.90 (t, 6H). ¹³C NMR (125 MHz, CDCl₃): δ(ppm) 159.84, 157.82, 153.00, 149.38, 143.24, 142.37, 137.08, 132.20, 131.00, 128.78, 125.02, 116.10, 113.20, 110.70, 31.64, 29.78, 29.72, 29.66, 29.60, 22.63, 14.11.

4,7-di(4-hexyl-5-bromo-thiophen-2-yl)-5,6-difluorine-2,1,3-benzothiadiazole (M4). **M4** was synthesized according to the similar route as **M2** with a yield as 4.3 g (78%). ¹H NMR (500 MHz, CDCl₃): δ(ppm) 7.96 (s, 2H), 2.65 (t, 4H), 1.68 (m, 4H), 1.32-1.41 (m, 12H), 0.90 (t, 6H). ¹³C NMR (125 MHz, CDCl₃): δ(ppm) 150.60, 148.48, 142.60, 131.71, 131.22, 114.47, 110.98, 31.64, 29.72, 29.56, 28.95, 22.64, 14.11.

Synthesis of the polymers. **M1** (62.8 mg, 0.055 mmol), **M2** (34.6 mg, 0.055 mmol) and 23 mL of anhydrous toluene were put into a 50 mL two-necked flask. The mixture was flushed with argon for 30 min. Then tris(dibenzylideneacetone)dipalladium(0) (Pd₂(dba)₃) (1.2 mg) and tri(o-tolyl)phosphine (P(o-Tol)₃) (1.5 mg) were added. The mixture was heated to 100 °C carefully, and vigorously stirred at this temperature for 24 h under argon atmosphere. After cooling down to room temperature, the solution was poured into 200 mL methanol. The polymer was collected by filtration

and was Soxhlet-extracted with methanol, hexane and chloroform, successively. The chloroform solution was concentrated to a small volume and dropped into methanol to precipitate out the polymer. After dried under vacuum at 50 °C overnight, the polymer **P1** was obtained as a blackish purple solid (26 mg, 37.1%). GPC (1,2,4-trichlorobenzene, polystyrene standard): $M_n = 31.0$ kDa, $M_w = 101.1$ kDa, PDI = 3.26. Anal. Calcd for $(C_{76}H_{102}N_2S_7)_n$ (%): C 71.92, H 8.04, N 2.21. Found (%): C 71.43, H 8.05, N 1.96.

P2 was obtained (59.5 mg, 84.1 %) according to the same route as **P1**. GPC (1,2,4-trichlorobenzene, polystyrene standard): $M_n=26.8$ kDa, $M_w=99.4$ kDa, PDI=3.71. Anal. Calcd for $(C_{76}H_{101}FN_2S_7)_n$ (%): C 70.92, H 7.85, N 2.17. Found (%): C 70.62, H 7.90, N 1.89.

P3 was obtained (50.7 mg, 70.0%) according to the same route as **P1**. GPC (1,2,4-trichlorobenzene, polystyrene standard): $M_n=24.2$ kDa, $M_w=90.2$ kDa, PDI=3.73. Anal. Calcd for $(C_{76}H_{100}F_2N_2S_7)_n$ (%): C 69.94, H 7.67, N 2.15. Found (%): C 69.78, H 7.74, N 2.00.

The M_w of **P3** was further controlled by increasing the reaction time to 36h and 48h to obtain 61.8 mg (86.2%) and 63.3 mg (87.4%) **P3**, corresponding M_w are 159.5 kDa (PDI=3.91) and 215.2 kDa (PDI=4.65), respectively.

2.2 Measurements

All compounds were characterized by nuclear magnetic resonance spectra (NMR) recorded on a Bruker AV 500 spectrometer in $CDCl_3$ at room temperature using tetramethylsilane as an internal reference at room temperature. The chemical shifts were accounted in ppm related to the singlet of $CDCl_3$ at 7.26 ppm and 77 ppm for 1H and ^{13}C NMR, respectively. Molecular weights and distributions of polymers were estimated by gel permeation chromatography (GPC) method, 1,2,4-trichlorobenzene as eluent and polystyrene as standard. Thermogravimetric analysis (TGA) of the polymers was investigated on a Universal V2.6D TA instruments. Differential scanning calorimetry (DSC) measurements were performed on a Mettler Toledo DSC1 star system at a heating rate of 20 °C min^{-1} under nitrogen. The absorption spectra were determined by a Unico UV-2102 scanning spectrophotometer. The electrochemical cyclic voltammetry was conducted on a CHI 660D Electrochemical Workstation with glassy carbon, Pt wire, and Ag/Ag^+ electrode as working electrode, counter electrode, and reference electrode respectively in a 0.1mol/L tetrabutylammonium hexafluorophosphate (Bu_4NPF_6) acetonitrile solution. Polymer thin films were formed by drop-casting chloroform solution (analytical reagent, 1mg/mL) onto the working electrode, and then dried in the air. Atomic force microscopy (AFM) images were collected in air under ambient conditions using the MultiMode scanning probe microscope (AFM, Veeco MultiMode V). Thickness of the active layer was measured on a Bruker Dektak-XT surface profiler.

2.3 Solvent vapour annealing

Solvent vapour annealing (SVA) was conducted at room temperature in a glove box. 3 ml THF was injected into a glass Petri dish which was closed for 1 min to let the THF vapour saturate the chamber. Then the as-cast film was transferred to the Petri dish. The film was about 1 cm above the solvent level during the solvent vapour annealing. After 30 sec, the film was removed from the treatment chamber.

2.4 Fabrication and characterization of PSCs

The device structure of the polymer solar cells was ITO/poly(3,4-ethylenedioxythiophene):poly(styrene sulfonic acid) (PEDOT:PSS, 40 nm)/polymer:[6,6]-phenyl-C71 butyric acid methyl ester ($PC_{71}BM$)/poly[(9,9-dioctyl-2,7-fluorene)-*alt*-(9,9-bis(3-N,N-dimethylamino)propyl)-2,7-fluorene] (PFN, 5 nm)/Al. The ITO glass was ultrasonically cleaned with detergent, distilled water, acetone, isopropyl alcohol, and then treated with ultraviolet-ozone (Ming Heng, PDC-MG) for 20 min. Then PEDOT:PSS (Clevios P VP AI 4083, H. C. Starck Inc.) was spin-coated from an aqueous solution onto the ITO substrates, followed by baking in air at 120 °C for 30 min on a hotplate. The substrates were transferred into a nitrogen filled glove box. The photoactive layer was prepared by spin-coating a blend solution of the polymer and $PC_{71}BM$ in *ortho*-dichlorobenzene (*o*DCB) on the top of ITO/PEDOT:PSS substrate (~80 nm). The sample was then thermally annealed at 80 °C for 10 min and solvent annealed for 30 sec. A 5 nm PFN layer was then spin-coated from methanol solution in presence of a trace amount of acetic acid onto the active layer. Subsequently, the films were transferred into a vacuum evaporator and Al was deposited as cathode. The effective area of a device was 0.16 cm^2 as determined by the shadow mask used during deposition of Al cathode. PCE values were determined from current density (J)-voltage (V) curve measurements (using a Keithley 2400 source meter) under 1 sun, AM 1.5G spectrum from a solar simulator (Newport model 94021A, 100 $mW\ cm^{-2}$). A monocrystal silicon cell (VLSI Standards Inc.) calibrated by the National renewable Energy laboratory (NREL) was used as a reference. The external quantum efficiency (EQE) of the devices was measured using a Hypermonolight System (QTEST 1000 AD, Crowntech Inc.).

2.5 Hole mobility measurement

The hole mobility was measured by the space-charge-limited current (SCLC) method in the hole-only device with a device structure of ITO/PEDOT:PSS/polymer: $PC_{71}BM/MoO_3/Al$ with the effective area of 0.16 cm^2 . The mobility was determined by fitting the dark current to the model of a single carrier SCLC, which is determined by the equation: $J = (9/8)\epsilon_0\epsilon_r\mu((V^2)/(d^3))$, where J is the current, μ is the zero-field mobility, ϵ_0 is the permittivity of free space, ϵ_r is the relative permittivity of the material, d is the thickness of the active layer, and V is the effective voltage. The effective voltage can be obtained by

Journal Name

ARTICLE

subtracting the built-in voltage (V_{bi}) and the voltage drop (V_s) from the substrate's series resistance from the applied voltage (V_{app}), $V = V_{app} - V_{bi} - V_s$. The hole mobility can be calculated from the slope of the $J^{1/2}$ - V curves.

2.6 Frequency dependent capacitance measurement

The capacitance (C) was obtained using impedance measurements at different frequency on a TOYO corporation EC-1 elastic constant measurement system at 25 °C, assuming an equivalent circuit of a capacitor in parallel with a resistor. Then the relative dielectric constant (ϵ_r) can be calculated from the equation: $C = \epsilon_0 \epsilon_r A/d$,^[23] where C is measured capacitance values, ϵ_0 is the vacuum dielectric constant (8.85×10^{-12} F m⁻¹), ϵ_r is the relative dielectric constant, A is the effective area of the blend film (0.16 cm²) which is defined by the shadow mask used during deposition of Al cathode, d is the thickness of the active layer (~80 nm).

3. RESULTS AND DISCUSSION

3.1 Materials design and synthesis

The three polymers, **P1**, **P2** and **P3** were synthesized by the typical Stille coupling polymerization of 2,6-bis(trimethyltin)-4,8-bis(2,3-diethylthiophen-5-yl)-benzo[1,2-b:4,5-b']dithiophene (**M1**) with three DTBT monomers: 4,7-di(4-hexyl-5-bromo-thiophen-2-yl)-2,1,3-benzothiadiazole (**M2**), 4,7-di(4-hexyl-5-bromo-thiophen-2-yl)-5-fluorine-2,1,3-benzothiadiazole (**M3**) and 4,7-di(4-hexyl-5-bromo-thiophen-2-yl)-5,6-difluorine-2,1,3-benzothiadiazole (**M4**) (Scheme 1). The monomers were readily prepared through modification routines according to the literature procedures^[9-11,19] and our previous work^[21] (Scheme 1). The molecular structures of the monomers were confirmed by ¹H NMR and ¹³C NMR. **P1**, **P2** and **P3** were purified by Soxhlet-extracted with methanol, hexane and chloroform subsequently. And then obtained by precipitated from methanol with a high yield (>84% for **P2** and **P3**), except a low yield of 37% for **P1** due to the loss to the extraction with hexane. All polymers showed excellent solubility in common organic solvents (chloroform, tetrahydrofuran, dichlorobenzene, etc) at room temperature. The gel permeation chromatography (GPC) using polystyrene as standard and 1,2,4-trichlorobenzene as eluent, showed that the number-average molecular weight (M_n) of **P1**, **P2** and **P3** are 31.0 kDa, 26.8 kDa, 40.8 kDa, and the corresponding weight-average molecular weight (M_w) are 101.1 kDa, 99.4 kDa and 90.2 kDa, respectively. Furthermore, prolonged

polymerization times were used to prepare two **P3** with higher M_w as 159.5 kDa (36h) and 215.2 kDa (48h), respectively.

3.2 Properties of the polymers

The thermal properties of these polymers were investigated by thermogravimetric analysis (TGA) and showed in Figure 1a. The corresponding 5% weight-loss temperature (T_d) were 435 °C for **P1**, 430 °C for **P2** and 443 °C for **P3**, respectively, under the inert atmosphere, indicating their good thermal stabilities. Differential scanning calorimetry (DSC) plots of the three polymers are shown in Figure 1b. No appreciable phase transition temperatures were observed. However, the melting peaks (T_m) could be found at 322 °C, 337 °C and 367 °C for **P1**, **P2** and **P3**, respectively, proving their good crystal structure^[24] at the heating process of the three polymers, especially the symmetric difluorinated polymer **P3**.

The optical absorption spectra of the three polymers were investigated both in chloroform and solid film as displayed in Figure 2a. All polymers exhibit a high-energy region absorption band in a range of 400-500 nm for the π - π^* transitions, and a low-energy region (500-750 nm) absorption band corresponding to the intermolecular charge transfer (ICT) between D and A units. In the solid states, the main absorption peaks of the three polymers all show red-shifted and broader absorption than those of in the solution, which means better planarity structure might be formed. And the absorption edges of the films are at 726 nm, 750 nm and 710 nm for **P1**, **P2** and **P3**, respectively, corresponding to the band gap (E_g) of 1.71 eV, 1.65 eV and 1.75 eV (Table 1). Therefore, introducing fluorine atoms into the DTBT unit can efficiently influence the optical band gaps of the resulting polymers.

To investigate the effect of fluorine substitutions on the frontier energy levels of the copolymers, cyclic voltammetry (CV) measurement was performed and shown in Figure 2b. The HOMO and the lowest unoccupied molecular orbital (LUMO) energy levels of the polymers were determined from the onset oxidation potentials (E_{ox}) and the onset reduction potentials (E_{red}) according to the following equations: $HOMO = -e(E_{ox} + 4.71)$ (eV); $LUMO = -e(E_{red} + 4.71)$ (eV), where the unit of potential is V vs Ag/Ag⁺.^[25] The HOMO and LUMO energy levels were obtained and listed in Table 1, in which the HOMO energy levels showed a decline trend along with the increased fluorine numbers, -5.09 eV for **P1**, -5.11 eV for **P2** and -5.13 eV for **P3**, separately. Because V_{oc} of BHJ PSCs is closely related to the gap between the HOMO level of the donor polymer and the LUMO level of the acceptor material in their blended films, higher V_{oc} can be anticipated in the PSCs based on the fluorinated polymers **P2** and **P3**.^[26] To make a clear

comparison, the energy levels diagrams of the used materials in the PSCs were summarized in **Figure 3**. The LUMO energy levels of the three polymers are significantly higher than that of PC₇₁BM, which ensure efficient electron transfer from the polymers to the PC₇₁BM.

Quantum chemistry calculation by the DFT (B3LYP/6-31G* level)^[27] method was performed to provide the electronic structures of the three polymers. Two repeat units were chosen as the model compounds for simulations of the three polymers, the side chains were kept without simplification to obtain the accurate results. As shown in **Figure 4**, the electron

density in HOMO orbitals distribute along the whole backbone despite somewhat more intensely at BDTT units and less at DTBT units. However, the electron density in LUMO orbitals are mainly localized at the DTBT units. The electron density distributions of the different orbitals imply that the internal charge transfers are possible in these D-A conjugated systems.^[28] It should be noted that the single or double F atoms that incorporated onto the DTBT units have significant effect on the HOMO and LUMO energy levels of **P2** (-4.92 eV/-2.63 eV) and **P3** (-4.99 eV/-2.64 eV) compared to the pristine

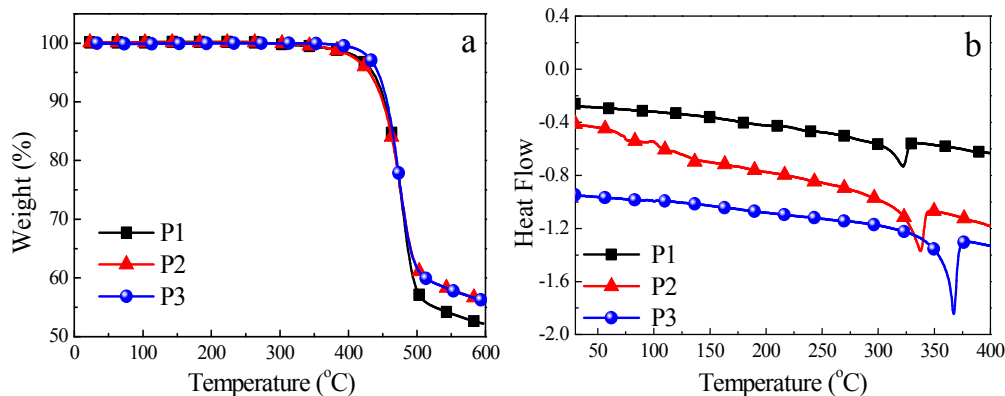


Figure 1 Thermalgravimetric analysis curves (a) and DSC (b) curves of **P1**, **P2** and **P3**.

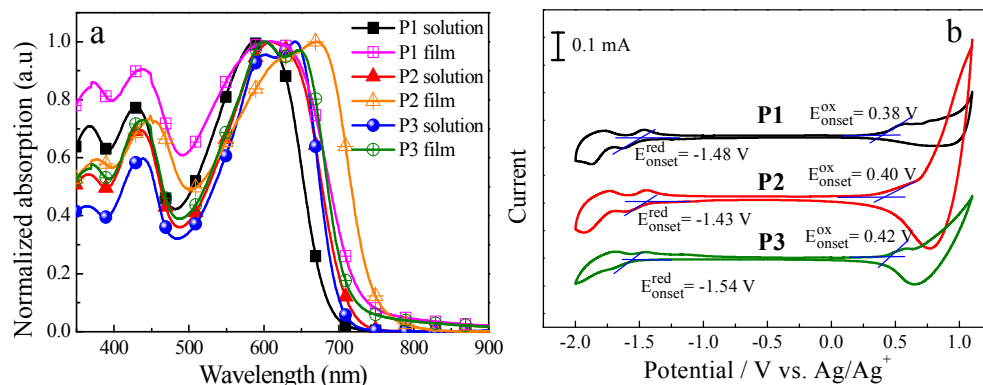


Figure 2. Absorption spectra of **P1**, **P2** and **P3** in solution and thin films (a); and Cyclic voltammograms of **P1**, **P2** and **P3** films on a glassy carbon electrode measured in 0.1 mol/L Bu₄NPF₆ solutions at a scan rate of 50 mV/s (b).

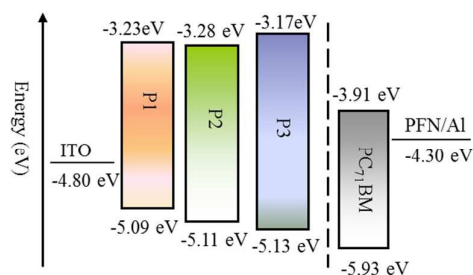


Figure 3. Schematic illustration of relative positions of HOMO/LUMO energy levels of the materials in the PSCs

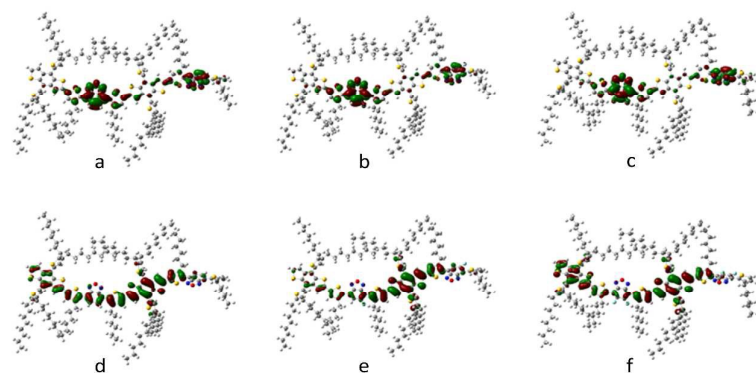


Figure 4. Calculated HOMO (a, b, c) and LUMO (d, e, f) distribution for **P1**(a, d), **P2**(b,e) and **P3** (c, f).

Table 1. Optical, electrochemical properties of the polymers

Polymer	λ_{edge} [nm]	$E_{\text{g}}^{\text{opta}}$ [eV]	HOMO ^{b)} [eV]	LUMO ^{b)} [eV]	$E_{\text{g}}^{\text{b)}$ [eV]	$E_{\text{red}}^{\text{c)}$ [V]	$E_{\text{ox}}^{\text{c)}$ [V]	HOMO ^{c)} [eV]	LUMO ^{c)} [eV]	$E_{\text{g}}^{\text{c)}$ [eV]
P1	726	1.71	-4.84	-2.57	2.27	-1.48	0.38	-5.09	-3.23	1.86
P2	750	1.65	-4.92	-2.63	2.29	-1.43	0.40	-5.11	-3.28	1.83
P3	710	1.75	-4.99	-2.64	2.35	-1.54	0.42	-5.13	-3.17	1.96

^{a)} estimated from the onset of electronic absorption of the polymer films ($E_{\text{g}}^{\text{opt}}=1240/\lambda(\text{nm})$). ^{b)} calculated results from the DFT at B3LYP/6-31G(d) level. ^{c)} cyclic voltammetry results.

polymer **P1** (-4.84 eV/-2.57 eV). The additional F atoms effectively depress the HOMO energy levels of the polymers, which agree well with the electrochemical results. The quantum chemistry calculation results were also listed in **Table 1**.

3.3 Characteristics and Optimization of Photovoltaic Devices

To investigate the photovoltaic properties, PSCs with a conventional device configuration of ITO/PEDOT:PSS/polymer:PC₇₁BM/PFN (5 nm)/Al, were fabricated in which PC₇₁BM as an acceptor. PFN was adopted as the cathode interface to improve the devices performance.^[29] Ortho-dichlorobenzene (oDCB) was chosen as the solvent for spin-coating blend films. A series of device with different polymer/PC₇₁BM ratio (wt/wt), 1:1, 1:2 and 1:3, were fabricated to investigate the photovoltaic performance. After coating of the active layer, thermal annealing (80 °C, 10 min) and THF solvent-annealing (SVA) 30 sec were utilized to optimize the phase separated morphology of blend films.^[30] The detailed results are listed in **Figure S1** and **Table S1** (ESI). Note that the devices from the **P1**, **P2** and **P3** exhibited their highest PCEs of 6.07%, 6.33% and 6.61% at the D/A ratio of 1:2 with similar J_{sc} and fill factors (FF), except for the enhanced V_{oc} of **P3** device (0.82V). To further improve the photovoltaic performance of **P3** based devices, D/A ratio of 1:1.5 was adopted and a superior PCE of 7.48% was achieved with higher

J_{sc} (12.7 mA cm⁻²) and V_{oc} (0.85 V). The enhanced V_{oc} values in the **P2** (0.79 eV) and **P3** (0.85 V) based devices are consistent with their deeper HOMO energy level. The current density-voltage characteristics (J - V) of these devices are shown in **Figure 5a** (AM 1.5G condition, 100 mW cm⁻²) and the device parameters are summarized in **Table 2**. The corresponding external quantum efficiency (EQE) curves of the devices with optimal donor: acceptor weight ratios are shown in **Figure 5b**. All devices exhibited a very broad response range from 400 to 700 nm. The **P1** and **P2** devices showed similar EQE profiles with high EQE responses at high energy region (410-530 nm), which might origin from the relatively high PC₇₁BM ratio in the active layers. Accordingly, the same J_{sc} was obtained for both devices (**Figure 5a**). However, enhanced EQE response in the low-energy region (550-700 nm) was achieved for the **P3** based device, suggesting that the photon-electron conversion process in this device at long wavelength was efficient.

To further improve the performance of **P3** based devices, two **P3** with higher molecular weight (MW) were synthesized through the prolonged polymerization times. The absorption spectra of the three **P3** both in solution and solid state films were exhibited in **Figure S2**. With the increasing MW, the absorption edges of **P3** films displayed steady red shift, from 710 nm for the low MW polymer ($M_{\text{w}}=90.2$ kDa, PDI=3.73) to 714 nm and further 722 nm for the medium MW ($M_{\text{w}}=159.5$ kDa, PDI=3.91) and high MW ($M_{\text{w}}=215.2$ kDa, PDI=4.65) **P3** films, respectively. Furthermore, C-V results as described in

Figure S3 and **Table S2** showed that the medium MW **P3** possessed relatively deep HOMO energy level (-5.14 eV) compared to other two **P3** polymers (-5.13 and -5.12 eV). *J-V* curves of the medium MW and high MW **P3**:PC₇₁BM based devices under optimal weight ratio (1:1.5) were shown in **Figure 5c** with the corresponding EQE in **Figure 5d**. The medium MW **P3** based device possessed the highest *J_{sc}* (14.1 mA cm⁻²) and best PCE of 8.16%. However, the high MW **P3** based device showed unexpectedly lowered *V_{oc}* (0.82 V), *J_{sc}* (11.7 mA cm⁻²) and FF (65.2%) in comparison to that of other two **P3** based devices, which gave rise to the lowered PCE (6.26%). The phenomenon that medium MW polymer based device displayed maximum photovoltaic parameters had been observed in the poly(3-hexyl)thiophene (P3HT):[6,6]-phenyl-C61 butyric acid methyl ester (PC₆₁BM) based devices.^[31] According to this literature, the poor performance of high MW polymer device might result from its relatively low solubility in the solvent, which would cause the unfavourable PCBM distribution. Moreover, for high MW **P3** in our work, the elevated HOMO energy level is also partially responsible for the low PCE.

Considering the promising photovoltaic properties of the medium MW **P3**, device optimization was further performed on this polymer by THF SVA incorporation with 3% (v/v) 1,8-

diiodooctane (DIO) and the corresponding *J-V* and EQE curves were also displayed in **Figure 5c** and **5d**. Despite its lowered *V_{oc}* (0.80 V) caused by the addition of DIO,^[32,33] the *J_{sc}* (14.8 mA cm⁻²) and FF (71.5%) were simultaneously improved, which resulted in an enhanced PCE of 8.47% and were in accord with the EQE response in the low-energy region (500-700 nm). It should be mentioned that the obtained PCE value (8.47%) among one of the best efficiencies achieved for BDTT and DTBT based polymers, verifying that **P3** with appropriate molecular weight should be promising polymer for highly efficient photovoltaic application.

3.4 Charge Transport, Dielectric Constant and Morphology Properties

As the hole mobility (μ_h) is crucial to achieve balance charge transport across the device, we used space-charge limited current (SCLC) method to measure the hole mobility in a device structure of ITO/PEDOT:PSS/polymer:PC₇₁BM/MoO₃/Al. As shown in **Figure 6a** and **Table 2**, the deduced hole mobility values of the three polymers (**P1**, **P2** and medium MW **P3**) were high and all about 1×10^{-4} cm²V⁻¹s⁻¹. After the addition of 3% DIO in the blend film (medium MW **P3**:PC₇₁BM=1:1.5), the

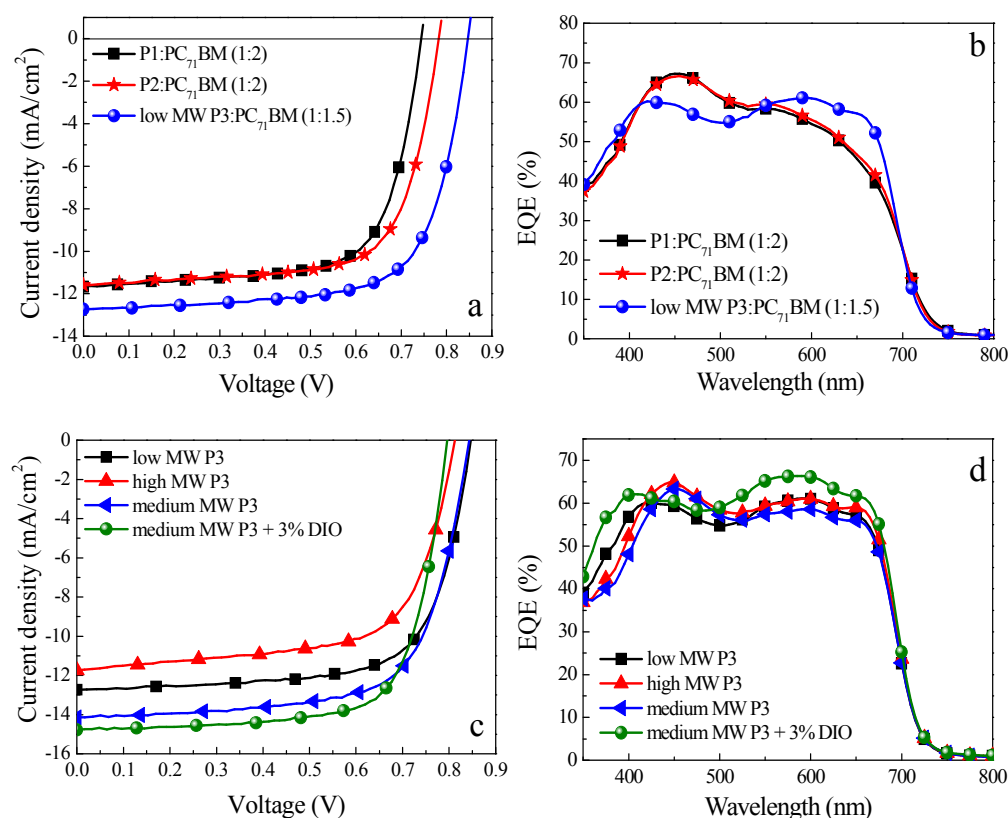


Figure 5 (a) *J-V* curves of the PSCs based on optimized **P1**, **P2** and **P3**/PC₇₁BM, under the illumination of AM 1.5G, 100mW/cm²; (b) EQE curves of the PSCs based on optimized polymer/PC₇₁BM ratio in oDCB; (c) *J-V* curves of the PSCs based on different MW **P3**/PC₇₁BM under optimal D/A ratio (1:1.5); (d) EQE curves of the PSCs based on optimized **P3** with different MW under optimal D/A ratio (1:1.5)

Journal Name

ARTICLE

hole mobility exhibited slightly increased, which was consistent with the observed high J_{sc} of the device as shown in **Table 2**.

V_{oc} of the polymer bulk heterojunction solar cells were not only determined by the energy difference between the HOMO energy level of the donor and the LUMO energy level of the acceptor, but also influenced by the dielectric constants of the blend films.^[22] We measured the capacitance values of **P1**, **P2** and medium MW **P3** based devices under their optimal condition and calculated the relative dielectric constants (ϵ_r) of the blending films at different frequency. The relative dielectric constants vs. frequencies were plotted in **Figure 6b**. The obtained ϵ_r for **P1**, **P2** and medium MW **P3** blending films

at 1 kHz were 3.31, 3.59 and 3.75, respectively, which were consistent with the high V_{oc} of the fluorinated polymers.

Atomic force microscopy (AFM) study was also carried out to investigate the phase-separated morphologies of the polymers:PC₇₁BM blends corresponding to the best performance, which were shown in **Figure 7**. The light and dark domains correspond to the aggregations of polymer and PC₇₁BM, respectively. All films exhibit interpenetrating feature with bicontinuous network with appropriate domain size (<20 nm) between polymer and PC₇₁BM. Furthermore, smooth surface with root-mean-square roughness (RMS) value of 0.96 nm for **P1**, 0.92 nm for **P2**, 1.21 nm for medium MW **P3** and 1.75 nm for the medium MW **P3** with 3% DIO blending films were investigated. These results are consistent in the high J_{sc} and FF of the BHJ PSCs.

Table 2 Optimal photovoltaic results of the PSCs based on polymer: PC₇₁BM under AM1.5G illumination (100 mW/cm²)

Polymer	Mn [kDa]	Mw [kDa]	PDI	Polymer:PC ₇₁ BM [w/w]	V_{oc} [V]	J_{sc} [mA cm ⁻²]	FF [%]	PCE _{max} (PCE _{ave} ±σ) ^{a)} [%]	μ_h (cm ² V ⁻¹ s ⁻¹)
P1	31.0	101.1	3.26	1:2	0.75	11.7	69.2	6.07(5.92±0.05)	1.27 × 10 ⁻⁴
P2	26.8	99.4	3.71	1:2	0.79	11.6	69.1	6.33(6.20±0.10)	1.00 × 10 ⁻⁴
Low MW P3	24.2	90.2	3.73	1:1.5	0.85	12.7	69.3	7.48(7.22±0.23)	/
Medium MW P3	40.8	159.5	3.91	1:1.5	0.85	14.1	68.1	8.16(8.02±0.10)	9.97 × 10 ⁻⁵
Medium MW P3	40.8	159.5	3.91	1:1.5(3%DIO)	0.80	14.8	71.5	8.47(8.35±0.19)	1.12 × 10 ⁻⁴
High MW P3	46.3	215.2	4.65	1:1.5	0.82	11.7	65.2	6.26(6.05±0.21)	/

^{a)} Calculated from 5 individual PSCs.

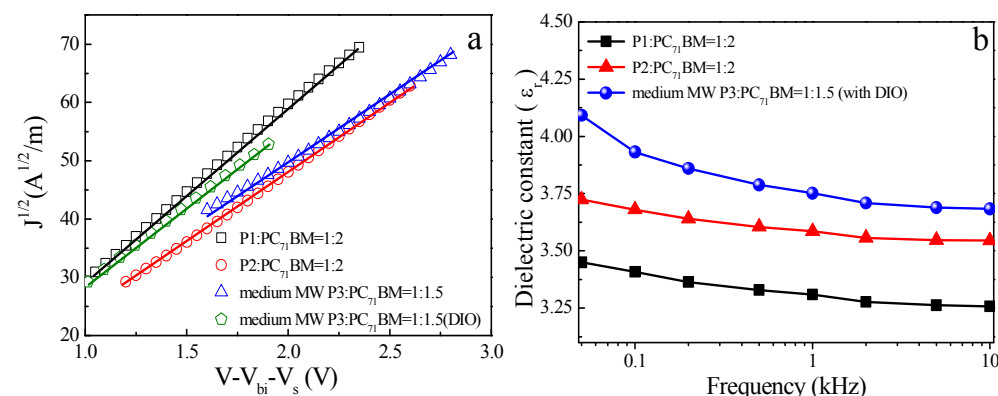


Figure 6. (a) $J^{1/2} \sim V$ characteristics of **P1**, **P2** and medium MW **P3** hole-only devices measured at ambient temperature; (b) dielectric constants calculated from capacitance for **P1**:PC₇₁BM 1:2 blend, **P2**:PC₇₁BM 1:2 blend as well as medium MW **P3**:PC₇₁BM 1:1.5 with 3% DIO blend, plotted as a function of frequency.

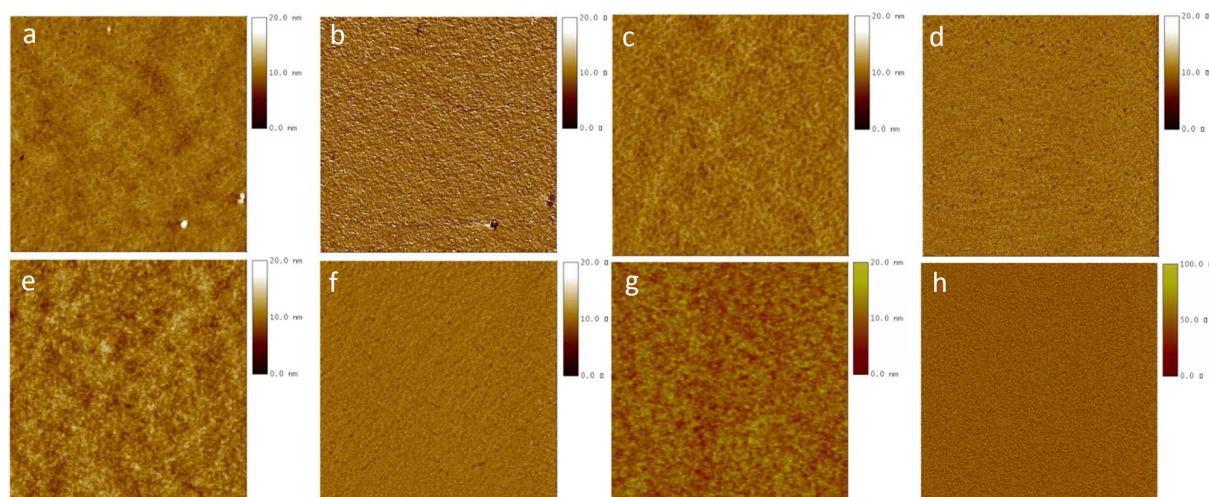


Figure 7. AFM height image and phase image ($5\mu\text{m}\times 5\mu\text{m}$) of **P1**:PC₇₁BM=1:2 (a, b), **P2**:PC₇₁BM =1:2 (c, d), medium MW **P3**:PC₇₁BM=1:1.5 (e, f); medium Mw **P3**:PC₇₁BM=1:1.5 with 3% DIO blend films (g, h).

4. CONCLUSION

Through introduction of proper side chain in the donor segment and spacer in the backbone, we have synthesized three 2D conjugated alternating copolymers of BDTT and fluorinated DTBT with good solubility. The addition of fluorine atoms on the electron-withdrawing unit have notable impacts on the properties of the polymers, including elevating the melt points, depressing the HOMO energy levels and increasing the relative dielectric constants. With these excellent basic parameters, a medium molecular weight two fluorine atoms substituted analogue **P3** shows fascinating power conversion efficiency as high as 8.47% in a conventional device, verifying that this polymer with appropriate molecular weight should be promising material for highly efficient photovoltaic application.

Acknowledgements

This work was supported by the National Natural Science Foundation of China (61274054, 21504067). The authors thank Prof. Jian Li of Xi'an Modern Chemistry Research Institute and Prof. Ergang Wang of Chalmers University of Technology for the assistance on DSC, dielectric constant and GPC measurements.

References

- [1] S.-H. Liao, H.-J. Jhuo, P.-N. Yeh, Y.-S. Cheng, Y.-L. Li, Y.-H. Lee, S. Sharma, S.-A. Chen, *Sci. Rep.*, 2014, **4**, 6813
- [2] (a) Y. Liu, J. Zhao, Z. Li, C. Mu, W. Ma, H. Hu, K. Jiang, H. Lin, H. Ade, H. Yan, *Nat. Commun.*, 2014, **5**, 5293. (b) J. Zhao, Y. Li, G. Yang, K. Jiang, H. Lin, H. Ade, W. Ma, H. Yan, *Nature Energy*, 2016, **1**, 15027
- [3] Z. He, B. Xiao, F. Liu, H. Wu, Y. Yang, S. Xiao, C. Wang, T. P. Russell, Y. Cao, *Nat. Photo.*, 2015, **9**, 174
- [4] X. Ouyang, R. Peng, L. Ai, X. Zhang, Z. Ge, *Nat. Photo.*, 2015, **9**, 520

- [5] M. Svensson, F. Zhang, S. C. Veenstra, W. J. H. Verhees, J. C. Hummelen, J. M. Kroon, O. Inganäs, M. R. Andersson, *Adv. Mater.*, 2003, **15**, 988
- [6] M. C. Scharber, D. Mühlbacher, M. Koppe, P. Denk, C. Waldauf, A. J. Heeger, C. J. Brabec, *Adv. Mater.*, 2006, **18**, 789
- [7] (a) N. Blouin, A. Michaud, M. Leclerc, *Adv. Mater.*, 2007, **19**, 2295; (b) J. Hou, H.-Y. Chen, S. Zhang, G. Li, Y. Yang, *J. Am. Chem. Soc.*, 2008, **130**, 16144; (c) C.-P. Chen, S.-H. Chan, T.-C. Chao, C. Ting, B.-T. Ko, *J. Am. Chem. Soc.*, 2008, **130**, 12828; (d) J. Hou, M.-H. Park, S. Zhang, Y. Yao, L.-M. Chen, J.-H. Li, Y. Yang, *Macromolecules*, 2008, **41**, 6012
- [8] (a) A. Gadisa, W. Mammo, L. M. Andersson, S. Admassie, F. Zhang, M. R. Andersson, O. Inganäs, *Adv. Funct. Mater.*, 2007, **17**, 3836; (b) Y. Lu, Z. Xiao, Y. Yuan, H. Wu, Z. An, Y. Hou, C. Gao, J. Huang, *J. Mater. Chem. C*, 2013, **1**, 630; (c) M. M. Wienk, M. Turbiez, J. Gilot, R. A. J. Janssen, *Adv. Mater.*, 2008, **20**, 2556; (d) Y. Liang, D. Feng, Y. Wu, S.-T. Tsai, G. Li, C. Ray, L. Yu, *J. Am. Chem. Soc.*, 2009, **131**, 7792; (e) A. Dhanabalan, J. K. J. van Duren, P. A. van Hal, J. L. J. van Dongen, R. A. J. Janssen, *Adv. Funct. Mater.*, 2001, **11**, 255
- [9] L. Huo, J. Hou, S. Zhang, H.-Y. Chen and Y. Yang, *Angew. Chem. Int. Ed.*, 2010, **49**, 1500
- [10] Q. Peng, X. Liu, D. Su, G. Fu, J. Xu, L. Dai, *Adv. Mater.*, 2011, **23**, 4554
- [11] H. Zhou, L. Yang, A. C. Stuart, S. C. Price, S. Liu, W. You, *Angew. Chem. Int. Ed.*, 2011, **50**, 2995
- [12] A. C. Stuart, J. R. Tumbleston, H. Zhou, W. Li, S. Liu, H. Ade, W. You, *J. Am. Chem. Soc.*, 2013, **135**, 1806
- [13] J. Lee, M. Kim, B. Kang, S. B. Jo, H. G. Kim, J. Shin, K. Cho, *Adv. Energy Mater.*, 2014, **4**, n/a
- [14] J. E. Carlé, M. Helgesen, N. K. Zawacka, M. V. Madsen, E. Bundgaard, F. C. Krebs, *J. Polym. Sci. B: Polym. Phys.*, 2014, **52**, 893
- [15] J.-H. Kim, S. A. Shin, J. B. Park, C. E. Song, W. S. Shin, H. Yang, Y. Li, D.-H. Hwang, *Macromolecules*, 2014, **47**, 1613
- [16] R. L. Uy, L. Yan, W. Li, W. You, *Macromolecules*, 2014, **47**, 2289
- [17] N. Wang, Z. Chen, W. Wei, Z. Jiang, *J. Am. Chem. Soc.*, 2013, **135**, 17060
- [18] X. Gong, G. Li, C. Li, J. Zhang, Z. Bo, *J. Mater. Chem. A*, 2015, **3**, 20195
- [19] M. Wang, X. Hu, P. Liu, W. Li, X. Gong, F. Huang, Y. Cao, *J. Am. Chem. Soc.*, 2011, **133**, 9638

- [20] L. Huo, S. Zhang, X. Guo, F. Xu, Y. Li, J. Hou, *Angew.Chem.Int. Ed.*, 2011, **50**, 9697
- [21] H. Wu, B. Zhao, W. Wang, Z. Guo, W. Wei, Z. An, C. Gao, H. Chen, B. Xiao, Y. Xie, H. Wu, Y. Cao, *J. Mater. Chem. A*, 2015, **3**, 18115
- [22] Y. Lu, Z. Xiao, Y. Yuan, H. Wu, Z. An, Y. Hou, C. Gao, J. Huang, *J. Mater. Chem. C*, 2013, **1**, 630
- [23] G. Zhang, T. M. Clarke, A. J. Mozer, *J. Phys. Chem. C*, 2016, **120**, 7033
- [24] J. Chen, L. Duan, M. Xiao, Q. Wang, B. Liu, H. Xia, R. Yang, W. Zhu, *J. Mater. Chem. A*, 2016, **4**, 4952
- [25] J. Hou, Z. Tan, Y. Yan, Y. He, C. Yang, Y. Li, *J. Am. Chem. Soc.*, 2006, **128**, 4911
- [26] G. Dennler, M. C. Scharber, T. Ameri, P. Denk, K. Forberich, C. Waldauf, C. J. Brabec, *Adv. Mater.* 2008, **20**, 579
- [27] a) R. Kroon, R. Gehlhaar, T. T. Steckler, P. Henriksson, C. Muller, J. Bergqvist, A. Hadipour, P. Heremans, M. R Andersson. *Sol. Energ. Mat. Sol C*. 2012, **105**, 280; b) G. K. Dutta, T. Kim, H. Choi, J. Lee, D. S. Kim, J. Y. Kim, C. Yang. *Polym.Chem*, 2014, **5**, 2540
- [28] X. Xu, Y. Wu, J. Fang, Z. Li, Z. Wang, Y. Li, Q. Peng. *Chemistry – A European Journal* 2014, **20**, 13259
- [29] (a) Z. He, C. Zhong, X. Huang, W. Wong, H. Wu, L. Chen, S. Su, Y. Cao. *Adv. Mater.* 2011, **23**, 4636. (b) Z. He, C. Zhong, S. Su, M. Xu, H. Wu, Y. Cao, *Nat. Photo.* 2012, **6**, 591
- [30] (a) J. Liu, L. Chen, B. Gao, X. Cao, Y. Han, Z. Xie, L. Wang. *J. Mater. Chem. A*, 2013, **1**, 6216; (b) G. L. Schulz, M. Löbert, I. Ata, M. Urdanpilleta, M. Lindén, A. Mishra, P. Bäuerle, *J. Mater. Chem. A*, 2015, **3**, 13738
- [31] W. Ma, J. Y. Kim, K. Lee, A. J. Heeger, *Macromo. Rapid. Commun.*, 2007, **28**, 1776
- [32] J. K. Lee, W. L. Ma, C. J. Brabec, J. Yuen, J. S. Moon, J. Y. Kim, K. Lee, G. C. Bazan, A. J. Heeger, *J. Am. Chem. Soc.*, 2008, **130**, 3619
- [33] J. Peet, J. Y. Kim, N. E. Coates, W. L. Ma, D. Moses, A. J. Heeger, G. C. Bazan, *Nat. Mater.*, 2007, **6**, 497